

TEXTURE ANALYSIS USING ADAPTIVE BIORTHOGONAL WAVELET PACKETS

G. C. K. Abhayaratne, Ian H. Jermyn, Josiane Zerubia

Ariana (CNRS/INRIA/UNSA joint research group)
INRIA, B.P. 93, 06902 Sophia Antipolis, France
email: charith@ieee.org, {Ian.Jermyn, Josiane.Zerubia}@inria.fr

ABSTRACT

We discuss the use of adaptive biorthogonal wavelet packet bases in a probabilistic approach to texture analysis, thus combining the advantages of biorthogonal wavelets (FIR, linear phase) with those of a coherent texture model. The computation of the probability uses both the primal and dual coefficients of the adapted biorthogonal wavelet packet basis. The computation of the biorthogonal wavelet packet coefficients is done using a lifting scheme, which is very efficient. The model is applied to the classification of mosaics of Brodatz textures, the results showing improvement over the performance of the corresponding orthogonal wavelets.

1. INTRODUCTION

The segmentation and classification of images based on texture analysis plays a major role in image understanding applications. Over the years, texture analysis has received considerable attention in terms of both methodology and application. The commonly used methods are based on statistical, model-based, and signal processing features.

In the signal processing approaches for texture analysis, feature extraction mainly includes two steps: the signal decorrelation step which usually consists of a signal transform and the computation of the feature metric, which is either an energy or a probability measure. The frequency domain energy distributions produced by the signal transforms are used to extract texture features. The commonly used transforms for texture analysis include Gabor transforms [1], ring and wedge transforms, wavelet transforms as wavelet packet decompositions [2, 3, 4] or wavelet frame decomposition [5]. For a comparative study on above techniques, see [6].

Most of the work on wavelet-based texture analysis has concentrated on orthogonal wavelets, which have the drawback that their design constraints do not allow the wavelet filter to be both FIR and linear phase, *i.e.* both real and symmetric. This can, however, be achieved for biorthogonal wavelets, where the analysis (primal) wavelet and the synthesis (dual) wavelet differ in length. It is well known that biorthogonal wavelets outperform orthogonal wavelets in

image coding. In this paper, we modify the approach to texture analysis presented in [4] to use biorthogonal wavelets, and then demonstrate their performance in texture classification experiments using Brodatz textures.

In section 2, we describe the adaptive probabilistic texture model using biorthogonal wavelets. Section 3 outlines the basics of biorthogonal wavelets, their lifting realization, and the mother wavelets used in the experiments. Section 4 shows the results of parameter estimation, and the classification of mosaics using Brodatz [7] textures. We conclude in section 5.

2. TEXTURE MODEL

The purpose of this section is to review the model described in [4] and to adapt it to use biorthogonal wavelets.

The model in [4] starts from a general translation invariant Gaussian distribution. The marginalized Gaussian distribution on an image region is then derived, and shown to be tractable if the original covariance lies in a certain class of operators. This class consists of those operators that are diagonal in at least one wavelet packet basis. The model is thus parameterized by a dyadic partition of the Fourier domain, which in conjunction with a mother wavelet defines a wavelet packet basis, and a function that assigns to each element of the partition (*i.e.* each subband), its variance. In [4], it is shown that exact MAP estimates of these parameters can be learned from samples of a texture using an efficient depth-first search algorithm on the space of dyadic partitions. The result is a model in which the basis adapts to the structure inherent in the texture according to a criterion derived from the texture model itself, rather than introduced on an *ad hoc* basis.

The Gaussian assumption might appear to go against the fact that the subband histograms of standard wavelet coefficients take on a leptokurtotic form more closely modelled by, for example, a generalized Gaussian with shape factor less than unity. However, most of these studies were concerned with 'natural' images. The statistics were thus comprised of mixtures of many components corresponding to different entities in the scene. There is no reason to suppose

The work of Dr. Abhayaratne was funded by the ERCIM postdoctoral fellowship programme.

that these statistics will be preserved for the images in a coherent texture class. Second, products of generalized Gaussians do not preserve their form under a change of basis, so that in a basis adapted to the texture class under consideration, again there is no reason to suppose that the statistics will necessarily assume the standard form. In the absence of more specific information, a Gaussian distribution is used as a maximum entropy choice: it supposes only that the energy in each of the adaptive subbands will be approximately preserved from texture sample to texture sample.

Following the line of argument used in [4], we can derive the expression for the model in terms of biorthogonal wavelets. The model is still characterized by a dyadic partition T and a function f on the partition, but now the probability distribution is given by:

$$\Pr(I|f, T) = \prod_{\alpha \in T} \left[\left(\frac{f_\alpha}{\pi} \right)^{\frac{N_\alpha}{2}} e^{-f_\alpha \sum_{i \in \alpha} w_{a_\alpha, i} w_{s_\alpha, i}} \right] \quad (1)$$

where I is the image; α indexes the subbands of T ; f_α is the value of f on subband α ; i indexes the wavelets within each subband; $w_{a_\alpha, i}$ and $w_{s_\alpha, i}$ are the (α, i) coefficients using the primal and dual wavelet bases B_α and B_s , respectively; and N_α is the number of pixels in the subband α .

MAP estimates of the parameters for a given texture are found by examining the probability of the parameters given a set of images $d = \{I_n\}$ of the texture:

$$\Pr(f, T|d) \propto \Pr(d|f, T)\Pr(f|T)\Pr(T) \quad (2)$$

We choose $\Pr(f|T)$ to be Jeffrey's ignorance prior. We choose the probability of a given partition T to be $\Pr(T) = Z^{-1}(\beta)e^{-\beta \sum_{t \in Q(T)} N_t}$ where $Q(T)$ is the quadtree naturally related to the partition, t is a vertex in this tree, and $N_t \propto 4^{-l(t)}$, where $l(t)$ is the depth of vertex t in the tree, is the size of the region of the Fourier domain corresponding to vertex t . The parameter β controls how severely the distribution penalizes large decompositions. Differentiating (1) with respect to f_α gives us the maximum a posteriori (MAP) estimate of f for a fixed T :

$$\hat{f}_\alpha = \frac{N_\alpha}{2 \sum_{i \in \alpha} |w_{a_\alpha, i} w_{s_\alpha, i}|} \quad (3)$$

A depth-first search through the space of dyadic decompositions allows us to find the MAP estimate for T efficiently.

2.1. Classification

In order to classify pixels, we use an undecimated wavelet decomposition, and consider the following approximation

to the exact probability distribution for the texture on a region R :

$$\Pr(I_R|f, T) = \prod_{\alpha \in T} \prod_{x \in R} \left[\left(\frac{f_\alpha}{\pi} \right)^{\frac{1}{2M_\alpha}} e^{-\frac{f_\alpha}{M_\alpha} \sum_{i \in \alpha} w_{a_\alpha, x} w_{s_\alpha, x}} \right] \quad (4)$$

where $M_\alpha = 4^{l(\alpha)}$ is the redundancy factor for subband α in the undecimated transform. The class of a pixel, $\lambda(x)$, is then estimated as:

$$\hat{\lambda}(x) = \arg \max_{l \in L} \Pr(I_{V(x)} | \lambda_{V(x)} = l) \quad (5)$$

where $V(x)$ is a set of neighbours of pixel x .

3. BIORTHOGONAL WAVELETS

For orthogonal wavelets, the synthesis mother wavelet filters are obtained by order flipping the analysis mother wavelet filters. Thus both analysis and synthesis mother wavelets are the same. For biorthogonal wavelets [8], different mother wavelet filters satisfying perfect reconstruction conditions can be chosen in the analysis and synthesis filter banks. The lifting scheme [9] is often used in designing and implementing biorthogonal wavelets. In this paper, we use a two-step lifting scheme to compute the biorthogonal wavelet packet coefficients, as described in the following sections.

3.1. The Lifting Scheme

The lifting scheme, first introduced as a method for wavelet design without using frequency domain techniques, forms a natural parameterization of the corresponding filter banks for spatial domain design and implementation. In addition, lifting yields in-place computation of the wavelet coefficients, thus enabling fast and memory efficient computations.

The basic idea of lifting is the factorization of the poly-phase matrix of the filter bank for a given wavelet transform into alternating upper and lower triangular matrices with unit diagonals. The general structure of a 1d lifting scheme consists of at least 4 steps: split, prediction lifting (P), update lifting (U), and normalization. The splitting for an input signal x^0 is:

$$\text{Split: } x_i = x_{2i}^0; \quad y_i = x_{2i+1}^0 \quad (6)$$

The prediction and update steps result in high-pass and low-pass channels respectively in the corresponding filter bank. Their order can be interchanged according to the scheme, as discussed in the following section.

3.2. Biorthogonal wavelets using lifting

We will use a class of biorthogonal wavelets known as interpolating wavelets [9], which can be realized using only

	M	\tilde{M}	l_a	l_s
(2,2)	2	2	3	5
(2,4)	2	4	3	9
(4,2)	4	2	7	9
(4,4)	4	4	7	13
Haar	1	1	2	2
D4	2	2	4	4
D8	4	4	8	8

Table 1. Details of the wavelets.

one prediction-update step. For such wavelets, the primal wavelet $|a\rangle$ is obtained using P+U lifting:

$$P: y'_i = y_i - \sum_{j=1-\lceil M/2 \rceil}^{\lfloor M/2 \rfloor} p_j x_{j+i} \quad (7)$$

$$U: x'_i = x_i + \frac{1}{2} \sum_{j=-\lfloor \tilde{M}/2 \rfloor}^{\lceil \tilde{M}/2 \rceil - 1} u_j y'_{j+i} \quad (8)$$

$$\text{Normalize: } x''_i = \sqrt{2}x'_i; \quad y''_i = y'_i/\sqrt{2} \quad (9)$$

where M and \tilde{M} are the number of vanishing moments in p and u respectively. Similarly, the dual wavelet $|s\rangle$ is obtained using U+P lifting:

$$U: x'_i = x_i + \sum_{j=1-\lceil M/2 \rceil}^{\lfloor M/2 \rfloor} p_j x_{j+i} \quad (10)$$

$$P: y'_i = y_i - \frac{1}{2} \sum_{j=-\lfloor \tilde{M}/2 \rfloor}^{\lceil \tilde{M}/2 \rceil - 1} u_j y'_{j+i} \quad (11)$$

$$\text{Normalize: } x''_i = x'_i/\sqrt{2}; \quad y''_i = \sqrt{2}y'_i \quad (12)$$

In both cases $\sum_j p_j = \sum_j u_j = 1$. Such wavelet pairs are usually denoted as (M, \tilde{M}) , where M (\tilde{M}) is the number of vanishing moments in the $|a\rangle$ ($|s\rangle$) mother wavelet.

Interpolating wavelets use interpolation filters for p and u . For example, two vanishing moments with coefficients $(\frac{1}{2}, \frac{1}{2})$ yields linear interpolation, while four vanishing moments with coefficients $(-\frac{1}{16}, \frac{9}{16}, \frac{9}{16}, -\frac{1}{16})$ yields cubic interpolation.

4. SIMULATION RESULTS

We present the performance of biorthogonal wavelets with vanishing moments (2,2), (4,2), (4,4), and (2,4), and compare them with orthogonal wavelets Haar, D4, and D8, which are the compact support wavelets with 1, 2, and 4 vanishing moments respectively. Table 1 summarizes the details of the wavelets used in these simulations, where l_a is the length of the primal mother wavelet and l_s the length of the dual mother wavelet.

The model we derived in section 2 reduces to that for orthogonal wavelets when the primal and dual bases are the same; thus we can use the model for orthogonal wavelets too.

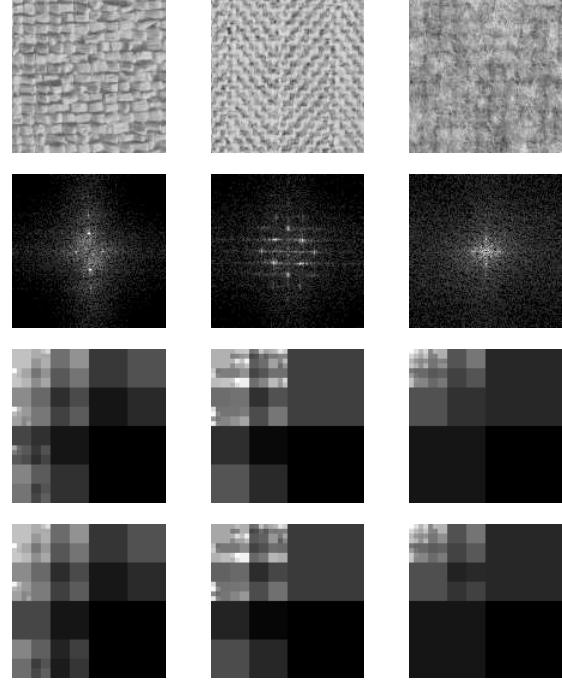


Fig. 1. Parameter estimation. Row 1: textures Raffia, Herring, and Wool; row 2: their power spectra; rows 3-4: their estimated parameters using (2,2) and (4,2) wavelets.

4.1. Parameter Estimation

The parameters T and f are estimated as described earlier. They are shown graphically in figure 1 for three textures: Raffia, Herring, and Wool; and two wavelets: (2,2) and (4,2). The brightness of each subband is proportional to $1/f_\alpha$.

4.2. Classification

We present the classification performance of the biorthogonal wavelet model using three synthetic mosaics of Brodatz textures. In figure 2, we show the test mosaics, M1, M2 and M3, the corresponding ground truth maps, and the misclassification maps, where the misclassified pixels are shown in black, for two different biorthogonal wavelets: (2,2) and (4,2).

The percentages of misclassified pixels are listed in table 2. It is evident from these results that for both orthogonal and biorthogonal wavelets, shorter mother wavelets with a smaller number of vanishing moments outperform longer mother wavelets with a larger number of vanishing moments. Moreover, we can compare the performance of the biorthogonal wavelet (2,2) with that of the orthogonal wavelet D4, since they have the same number of vanishing moments in both primal and dual wavelets (2 each), and they are the

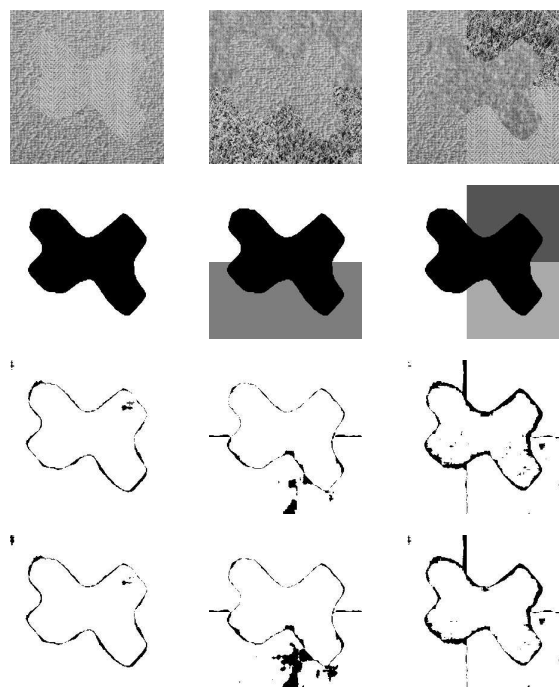


Fig. 2. Classification results. Row 1: mosaics M1, M2 and M3; row 2: ground truth; rows 3-4: misclassified pixels (in black) for classifications using (2,2) and (4,2) wavelets.

compact support wavelets for that vanishing moment pair in orthogonal and biorthogonal wavelets, respectively. As can be seen in table 2, the (2,2) wavelet outperforms the D4 wavelet for the mosaics: M1 and M3, and on average for the three mosaics. Similar performance can be seen for the biorthogonal and orthogonal wavelets with 4 vanishing moments, (4,4) and D8.

5. CONCLUSIONS

In this paper, we have presented an adaptive probabilistic texture model based on biorthogonal wavelets, and used it for texture classification and analysis. In this model, both the primal and the dual wavelets associated with a specific biorthogonal wavelet transform are used in the energy computation, in parameter estimation, and for classification. For both orthogonal and biorthogonal wavelets, shorter wavelets with fewer vanishing moments classify better than longer wavelets with more vanishing moments. The biorthogonal wavelets (2,2) and (4,4) resulted in better classifications compared to the corresponding compactly supported orthogonal wavelets with the same number of vanishing moments, D4 and D8. The use of the lifting scheme in this model provides very fast computation, in both training and classification, and also a parameterization of the wavelet filters

	M1	M2	M3	Average
(2,2)	2.637	3.333	6.736	4.235
(2,4)	2.675	4.720	6.783	4.726
(4,2)	2.829	5.770	6.058	4.886
(4,4)	2.827	7.598	6.073	5.499
Haar	2.178	2.533	6.163	3.625
D4	6.575	2.181	29.343	12.700
D8	4.631	3.384	22.031	10.015

Table 2. Percentages of misclassified pixels.

that we plan to use in future work to optimize the mother wavelet for a given texture, in addition to frequency domain decomposition.

References

- [1] A. K. Jain and F. Farrokhnia, "Unsupervised texture segmentation using gabor filters," *Pattern Recognition*, vol. 24, no. 12, pp. 1167–1186, 1991.
- [2] T. Chang and C.-C. J. Kuo, "Texture analysis and classification with tree structured wavelet transform," *IEEE Trans. Image Processing*, vol. 2, no. 4, pp. 429–441, 1993.
- [3] A. Laine and J. Fan, "Texture classification by wavelet packet signatures," *IEEE Trans. Patt. Anal. Mach. Intell.*, vol. 15, no. 11, pp. 1186–1190, 1993.
- [4] K. Brady, I. Jermyn, and J. Zerubia, "Texture analysis: An adaptive probabilistic approach," in *Proc. IEEE ICIP*, 2003, vol. 2, pp. 1045–1048.
- [5] M. Unser, "Texture classification and segmentation using wavelet frames," *IEEE Trans. Image Processing*, vol. 4, no. 11, pp. 1549–1560, 1995.
- [6] T. Randen and J. H. Husoy, "Filtering for texture classification: A comparative study," *IEEE Trans. Patt. Anal. Mach. Intell.*, vol. 21, no. 4, pp. 291–309, 1999.
- [7] P. Brodatz, *Textures: A Photographic Album for Artists and Designers*, Dover, New York, USA, 1966.
- [8] A. Cohen, I. Daubechies, and J.-C. Feauveau, "Biorthogonal bases of compactly supported wavelets," *Comm. Pure Appl. Math.*, vol. 45, no. 5, pp. 485–560, 1992.
- [9] W. Sweldens, "The lifting scheme: A custom-design construction of biorthogonal wavelets," *Appl. Comput. Harmon. Anal.*, vol. 3, no. 2, pp. 186–200, 1996.